Multipole Moments of the CPT Density Matrix in Polarization Modulation Conditions

Zachary Warren and James Camparo
Physical Sciences Laboratories
The Aerospace Corporation
El Segundo, CA, USA

***Summary*—Current compact atomic clock technologies rely on coherent population trapping (CPT), which employs a microwave resonance to stabilize a crystal oscillator. Standard CPT, while a simple and easy-to-implement optical preparation scheme in alkali metal atoms, suffers from low signal-to-noise ratios (SNR). The primary contributor to the low signal amplitude is the collection of atoms at the extreme ends of the Zeeman sublevels in the hyperfine levels of the alkali ground state, so-called "trap states." Solutions to the trap-state problem have been reported previously, though the redistribution of atomic population into the CPT signal states with these methods has not yet been carefully examined. This work aims to provide an experimental basis to evaluate trap-state recovery schemes.**

Keywords—coherent population trapping; multipole moments; atomic clock; polarization; density matrix

I. INTRODUCTION

Precise timekeeping within size, weight, and power (SWaP) constrained systems, such as satellites, requires clocks and oscillators that fit within a tight SWaP budget. Chip-scale atomic clocks (CSACs) are a common consideration to meet this need, though they come at a significant tradeoff in performance compared to other atomic clocks.

One of the primary contributors to the limitation in clock performance of the CSAC is the device's signal-to-noise ratio (SNR). CSACs typically use coherent population trapping (CPT) for clock signal generation due to its simplicity and elimination of a microwave cavity surrounding the alkali metal vapor cell. In our studies, CPT is demonstrated with ^{87}Rb vapor and a vertical cavity surface emitting laser (VCSEL) diode.

With standard CPT, the atomic signal is generated with circularly polarized light, which results in some atoms becoming stuck in the extreme end states of the ground-state hyperfine levels' Zeeman sublevels (*i.e.*, "trap states"). This process prevents those trap-state atoms from contributing to CPT, thereby limiting the available population for clock signal generation. There have been several studies on the effect of spin-exchange and spin polarization in atomic vapors, even in terms of multipoles, though not utilizing state multipoles as a metric determining optimal population distributions for CPT [1,2].

Through evaluation of the population distribution via state multipole analysis, we can validate and optimize diverse trap-state recovery methods for overall improvement of CSAC designs. We have reported on this test setup and methodology previously [3,4], and present here new data with improved analysis. Our present focus is on the trap-state recovery method utilizing dual (or double) polarization and phase modulation, which was a scheme first described by Yun *et al* (2014) [5].

II. METHODS

CPT requires two fields that coherently couple the upper and lower alkali ground-state hyperfine levels to a common excited state. For our experiments, the standard bi-modal (pump) field of a modulated laser is complimented by a second probe laser. The two laser beams are colinear in a vapor cell. The pump laser is phase modulated at 3.4 GHz, with CPT produced through optical excitation of Rb by the two first order optical sidebands (known as a Λ system). The probe is low power and tunable, and is used to measure the monopole, dipole, and quadrupole moments of the ground-state population distribution in each of the ground-state hyperfine manifolds.

With the pump laser circularly polarized, conservation of angular momentum during the excitation/spontaneous-decay process transfers angular momentum from the pump laser to the atomic vapor, resulting in population accumulation in the Zeeman end states (*e.g.,* $m_F = \pm 2$). This in turn reduces the clock signal amplitude by limiting the population available to the $m_F=0 - m_F=0$ CPT transition. The end states are not coupled to excited states for this optical polarization as shown in Fig. 1 (left): atoms are trapped in the Zeeman end state. Alternating the angular momentum of the pump laser via polarization modulation, Fig. 1 (right), results in redistribution of the ground state population. Unfortunately, this method to recover atoms from the trap state produces a CPT doublet, despite reintroducing the atom population into the $m_F=0 - m_F=0$ system – the two Λ systems do not constructively add [6].

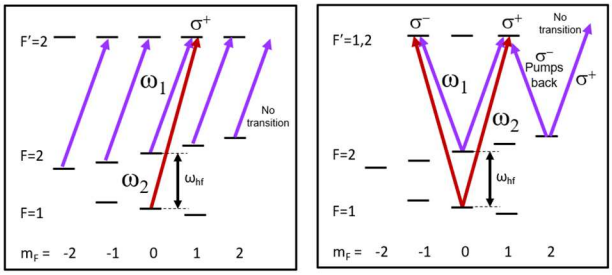

Figure 1 Laser pumping schemes for single polarization at left and polarization modulation at right (transitions from F_g=1 and states in F_e = 1 are not shown)

Approved for public release. OTR 2022-00612.

To recombine the CPT doublet under polarization modulation into a single CPT resonance, a research team at SYRTE introduced synchronous phase modulation to the method, which collapsed the doublet and resulted in improved SNR of the CPT signal [5]. This dual-modulation method to increase CPT SNRs therefore has significant potential, and it is the purpose of the research program we have instituted to better understand the underlying physics of dual-modulation in atomic vapors. As in our previous studies to quantify ground-state population distributions, we consider a state multipole description of the ground-state density matrix as modified by the light-matter interaction [7].

To measure the state multipoles in CPT, we use a distributed feedback (DFB) laser and a VCSEL described earlier to launch light through a vapor cell containing ^{87}Rb, shown in Fig. 2. The DFB probe laser was attenuated to 20 nW of total optical power to eliminate any potential of optical pumping and chopped for detection separate from the pump via a lock-in amplifier. Each laser has independent adjustable polarizations for the range of tests we perform. The modulated VCSEL generates CPT, while the single frequency DFB laser is tuned over the rubidium absorption spectrum. For later reference we note that the integral of the full absorption spectrum is proportional to $NLpr_ofc$, where N is the number density of ^{87}Rb atoms in the vapor, r_o is the classical electron radius, f is the oscillator strength for the D_1 Rb resonance, and L is the vapor length.

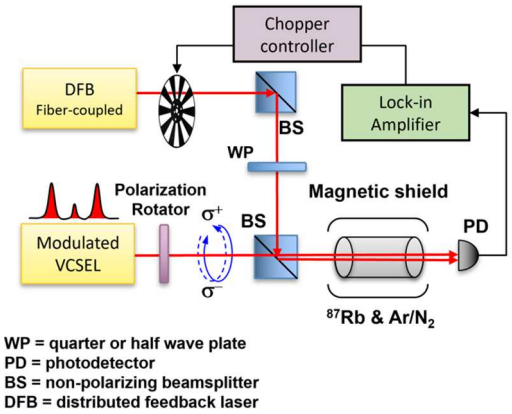

Figure 2 Test setup includes a microwave-modulated VCSEL to prepare CPT and a DFB probe, optically chopped for lock-in detection signal; and a polarization switch (rotator)

In Table I, we have defined the experimentally assessable state multipoles, and the coefficients are also derived by others [8]: when there is no coherence among ground state sublevels, the state multipoles can be labelled as g_L, where the subscript L indicates the state multipole order: monopole (L = 0), dipole (L = 1), quadrupole (L = 2), etc. For the purposes of measurement and subsequent calculation, we define η_F as the fractional population in a ground-state hyperfine level, $\langle F_z \rangle$ as the orientation of azimuthal angular-momentum in a specific ground-state hyperfine level, and $\langle Q_F \rangle$ as the quadrupole moment of azimuthal angular momentum in a specific hyperfine level.

To acquire physically meaningful values, the measurement is performed in successive stages. First, the modulated VCSEL diode is prepared in one of four possible cases: 1) off-resonance from CPT, 2) at the peak of standard CPT, 3) at the peak of polarization-modulation CPT, and 4) at the peak of dual-polarization-and-phase modulation CPT. For any specific scenario the DFB probe laser is then tuned over the rubidium absorption spectrum twice: once with the probe polarization aligned vertically to the atoms' quantization axis, and once with circular probe polarization relative to the atoms' quantization axis.

TABLE I. DEFINITION OF MULTIPOLE MOMENTS

Multipole Moment	$F_g = 1$	$F_g = 2$
g_0	$\frac{\eta_F}{\sqrt{3}}$	$\frac{\eta_F}{\sqrt{5}}$
g_1	$\frac{\langle F_Z \rangle}{\sqrt{2}}$	$\frac{\langle F_Z \rangle}{\sqrt{10}}$
g_2	$\frac{\langle Q_F \rangle}{\sqrt{6}}$	$\frac{\langle Q_F \rangle}{3\sqrt{14}}$

For all eight cases, we integrate various resonances associated with the absorption spectrum and then normalize to $NLpr_ofc$. These are shown as a,b and c,d in Fig. 3. The attenuation coefficients (*i.e.*, NσL) are calculated as $ln(I_0/I)$=NσL where I_0 is the background light and I is the signal. Using vertical polarization of the probe, we first determine the fractional population η, and then through circular polarization of the DBR determine the orientation of the azimuthal angular momentum $\langle F_z \rangle$. (Determination of quadrupole moments requires analysis that differentiates the excited state hyperfine splitting in the spectra, which will be discussed in a future report.)

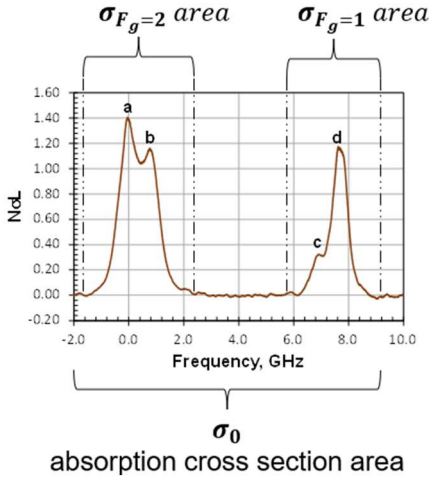

Figure 3 Absorption spectrum for a laser tuned to the D1 transition of ^{87}Rb. A "pump" laser generates a CPT signal, and a weak probe laser is used to investigate the ground-state hyperfine-level population distribution created by the pump laser. Ground state absorption cross section areas are defined.

The calculation thus takes on the form where the probe laser is set to linearly polarized light:

$$\sigma_{F_g=1} = \eta_{F_g=1}\ \sigma_0 \quad (1)$$

and

$$\sigma_{F_g=2} = \eta_{F_g=2}\ \sigma_0 \quad (2)$$

The ratio of the areas (a & b) and (c & d) to NLpr$_o$fc gives the fractional population η_{F_g}. With the probe laser circularly polarized, and knowing η_{F_g}

$$\sigma_{F_g=1} = \left(\eta_{F_g=1} + \frac{1}{2}\langle F_z\rangle\right)\sigma_0 \quad (3)$$

and

$$\sigma_{F_g=2} = \left(\eta_{F_g=2} - \frac{1}{2}\langle F_z\rangle\right)\sigma_0 \quad (4)$$

Now, the ratio of the areas (a & b) and (c & d) to NLpr$_o$fc yields information on the angular momentum orientation $\langle F_z\rangle$.

III. RESULTS

Through minimization of the probe's optical power to reduce the amount of optical pumping by the probe laser, a spectrum was produced for the relevant test parameters under varying polarization conditions. Because of the reduction in pumping, the values calculated from this data are expected to indicate the distribution more clearly.

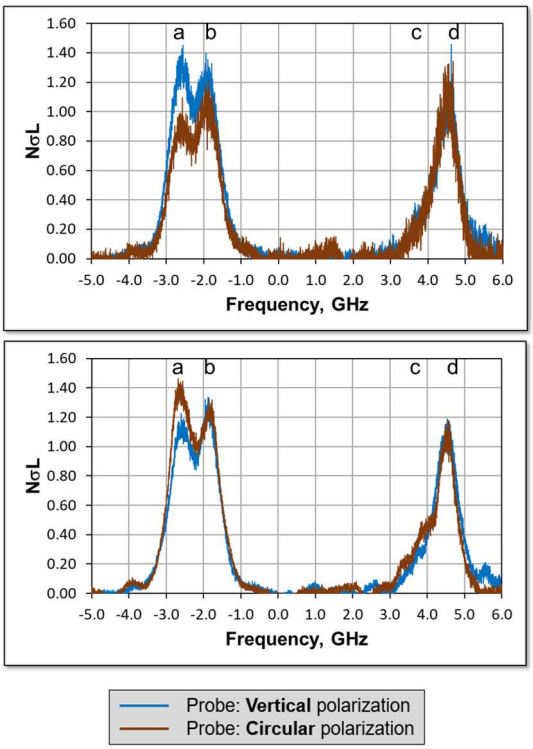

Figure 4 Upper: while the VCSEL pump prepares traditional single polarization CPT, the DFB laser probe scans over the rubidium spectra while vertically polarized (background/blue), or circularly polarized (foreground/red). Lower: pump prepares CPT with dual modulation, with same probe scheme.

In Figure 4, the probe was tuned over the rubidium resonances with its two different polarization states: vertical (background/blue) and circular (foreground/red). The top figure in Fig. 4 was collected while the pump prepared CPT with circular polarization in the traditional method, and the bottom figure was collected while the pump prepared CPT with polarization modulation in combination with phase switching.

The fractional population h in each of the hyperfine levels was calculated using the method in section II and shown for each case and hyperfine ground level in Fig. 5. As expected, the overall population distribution remained around 3/8 for the lower hyperfine level (due to the three Zeeman sublevels) and the upper hyperfine level maintained about 5/8 for its five Zeeman sublevels. The average azimuthal angular momentum $\langle F_z\rangle$ for each of the hyperfine levels was also calculated and shown in Fig. 6 for each CPT preparation condition.

The figures showing h and $\langle F_z\rangle$ demonstrate that polarization modulation and DM-CPT significantly decrease $\langle F_z\rangle$ compared to standard CPT and consequently the fractional population in the Zeeman end states. Given there remains some non-zero $\langle F_z\rangle$ for both polarization modulation and DM-CPT, this may be attributed to slightly non-optimum CPT modulation parameters, leaving an area for investigation in the next studies.

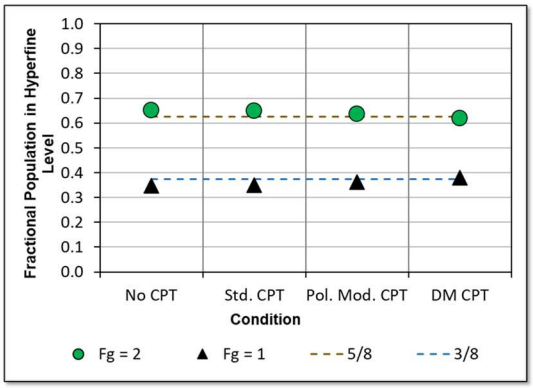

Figure 5 Experiment result demonstrates fractional population distributions in the two hyperfine ground states are evenly distributed in each atomic resonance preparation condition

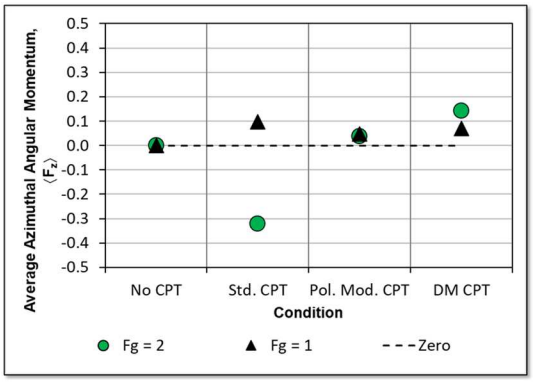

Figure 6 Through analysis of the rubidium spectra, the relative orientation of the atomic populations within the two hyperfine ground states is expressed as angular momentum states, showing a significant change between standard CPT and the polarization modulation methods

IV. DISCUSSION

As expected, in the absence of CPT pump, net azimuthal angular momentum is not imparted to the hyperfine states, while traditional CPT preparation does produce an overall spin polarization in the vapor due to conservation of angular momentum as the atoms absorb circularly polarized photons from the bi-modal CPT field. When polarization modulation is applied to the laser light, $\langle F_z \rangle$ returns to nearly 0. Similarly with dual modulation the behavior is nearly the same. The offset from exactly zero in the present data is likely due to the single measurement and insufficiently prepared modulation characteristics, which will be fine-tuned in future studies.

V. CONCLUSIONS

In order to optimize trap-state mitigation strategies in CPT, and identify parameters that crucially influence those mitigation strategies, it will be necessary to carefully study ground-state population distributions. Our work is aimed at initiating those studies by quantifying ground-state population distributions via three density-matrix multipole moments for each hyperfine level: the monopole, dipole, and quadrupole moments. This is achieved in a CPT-Pump/Probe experimental arrangement.

In future work we plan to analyze the atomic spectra with a Voigt profile to disentangle excitation to the two excited-state hyperfine levels. This will allow us to extract quadrupole moment information from the spectra. Through this work, a more complete view of CPT population distributions can be made and enable this method to be used as a tool for CPT performance enhancement in compact atomic clocks.

REFERENCES

[1] Y. Shi, T. Scholtes, Z. D. Grujić, V. Lebedev, V. Dolgovskiy, and A. Weis, “Quantitative study of optical pumping in the presence of spin-exchange relaxation,” Phys. Rev. A 97, 013419 (2018).

[2] J. Xu, G. Wäckerle, and M. Mehring, “Optical detection of spin multipole order in the ground state of alkali atoms,” Z Phys D - Atoms, Molecules and Clusters 42, 5–13 (1997).

[3] Z. Warren and J. Camparo, "Measuring Multipole Moments of the CPT Density Matrix Under Optical Field Polarization-Modulation Conditions," Proceedings of the 53rd Annual Precise Time and Time Interval Systems and Applications Meeting, Long Beach, California, January 2022, pp. 80-86.

[4] Z. Warren, J. Camparo, "Measuring multipole moments of the CPT density matrix during optical polarization modulation," Proc. SPIE 12016, Optical and Quantum Sensing and Precision Metrology II, 1201605 (2022).

[5] P. Yun, J.-M. Danet, D. Holleville, E. de Clercq, and S. Guérandel, “Constructive polarization modulation for coherent populating trapping clock,” Appl. Phys. Lett. 105, 231106 (2014).

[6] M. Huang and J. C. Camparo, Coherent population trapping under periodic polarization modulation: Appearance of the CPT doublet, Phys. Rev. A 85, 012509 (2012).

[7] K. Blum, Density Matrix Theory and Applications (Plenum Press, New York, 1981).

[8] D. Budker, D. F. Kimball, and D. P. DeMille, Atomic Physics (Oxford University Press, Oxford, UK 2008).